Exp. Anim. 63(3), 311–319, 2014

—Original—

In Vivo image Analysis Using iRFP Transgenic Mice

Mai Thi Nhu TRAN[1,3)]*, Junko TANAKA[2)]*, Michito HAMADA[1,3)], Yuka SUGIYAMA[2)], Shota SAKAGUCHI[2)], Megumi NAKAMURA[1)], Satoru TAKAHASHI[1,3)], and Yoshihiro MIWA[2)]

[1)]*Department of Anatomy and Embryology, University of Tsukuba, 1-1-1, Tennodai, Tsukuba, Ibaraki 305-8575, Japan*
[2)]*Department of Molecular Pharmacology, University of Tsukuba, 1-1-1, Tennodai, Tsukuba, Ibaraki 305-8575, Japan*
[3)]*International Institute for Integrative Sleep Medicine (WPI-IIIS), University of Tsukuba, 1-1-1, Tennodai, Tsukuba, Ibaraki 305-8575, Japan*

Abstract: Fluorescent proteins with light wavelengths within the optical window are one of the improvements in *in vivo* imaging techniques. Near-infrared (NIR) fluorescent protein (iRFP) is a stable, nontoxic protein that emits fluorescence within the NIR optical window without the addition of exogenous substrate. However, studies utilizing an *in vivo* iRFP model have not yet been published. Here, we report the generation of transgenic iRFP mice with ubiquitous NIR fluorescence expression. iRFP expression was observed in approximately 50% of the offspring from a matings between iRFP transgenic and WT mice. The serum and blood cell indices and body weights of iRFP mice were similar to those of WT mice. Red fluorescence with an excitation wavelength of 690 nm and an emission wavelength of 713 nm was detected in both newborn and adult iRFP mice. We also detected fluorescence emission in whole organs of the iRFP mice, including the brain, heart, liver, kidney, spleen, lung, pancreas, bone, testis, thymus, and adipose tissue. Therefore, iRFP transgenic mice may therefore be a useful tool for various types of *in vivo* imaging.
Key words: fluorescent protein, *in vivo* imaging, iRFP, optical window

Introduction

The first fluorescent protein, green fluorescent protein (GFP) was isolated from *Aequorea victoria* jellyfish in 1962 [3]. Thereafter, many fluorescent proteins were discovered or generated, and have provided considerable benefits to researches. Fluorescent proteins have been used to identify and track a target gene's activity in living cells, investigate and evaluate tumor progress, identify bacterial and viral infections, and observe cell migration within a host [6]. *In vivo* molecular imaging is an essential tool for detecting target biomolecules directly, and non-invasively and for visualizing molecular processes. However, observing conventional fluorescent proteins in deep tissue is difficult because of absorbance by hemoglobin and skin melanin.

The optical window is the wavelength range in which light can penetrate biological tissues. However, the optical window is limited because of absorption by water at wavelengths above 1,100 nm and by hemoglobin and melanin at wavelengths below 600 nm. Thus, the near-infrared light from ~650 to 900 nm is the optimal light range for the optical window [2].

Infrared fluorescent protein 1.4 (IFP1.4) is the first near-infrared fluorescent protein that has been used for *in vivo* imaging [4]. IFP1.4 is a fluorescent mutant of *Dr*BphD bacteriophytochrome from *Deinococcus radiodurans*. Bacteriophytochrome consists of two chains: a

(Received 24 December 2013 / Accepted 21 February 2014)
Address corresponding: Y. Miwa, Department of Molecular Pharmacology, University of Tsukuba, 1-1-1, Tennodai, Tsukuba, Ibaraki 305-8575, Japan
**M.T.N.T and J.T. are contributed equally to this work.*

PAS domain and a GAF domain. When these domains covalently bind to a chromophore, such as biliverdin IX α (BV), this complex can absorb red light. Biliverdin is an endogenous product of heme catabolism. However, endogenous biliverdin is insufficient for maximal fluorescence expression in mammalian cells [4]. Thus, the addition of exogenous biliverdin is required to achieve sufficient infrared fluorescence intensity. Recently, Filonov *et al.* generated a new infrared fluorescent protein, iRFP [1]. This protein is a fluorescent mutant of *Rp*BphP2 bacteriophytochrome from *Rhodopseudomonas palustris*. This protein can be excited at 690 nm and emits fluorescence at 713 nm. Transient overexpression of iRFP caused bright fluorescence in cells, tissues and the entire animal body without the addition of exogenous biliverdin. In addition, iRFP is more stable, brighter, and stronger compared with IFP1.4 [1]. Nevertheless, experiments using an iRFP transgenic model have not been reported. Here, we have established iRFP transgenic mice with ubiquitous red light emission.

Materials and Methods

Generation of iRFP transgenic mice

iRFP cDNA was amplified from pUC57-iRFP (a gift from the DNA distribution service from the "Fluorescence Live Imaging" Grant-in-Aid for Scientific Research on Innovative Areas) using primers containing a 5′ KOZAK sequence and a 3′ stop codon; the cDNA was subsequently cloned into the pEB6CAGMCS plasmid [5]. iRFP transgenic mice were produced by microinjecting *Spe* I/*Afl* II-digested DNA (carrying the CAG promoter − iRFP cDNA − SV40 polyA construct) into fertilized C57BL/6J (Japan SLC) eggs using standard procedures. The genotypes were determined by PCR analysis of tail DNA. The sequences of the forward and reverse primers were 5′ cctacagctcctgggcaacgtgctgg 3′ and 5′ gcggcctgcaggcgcctga 3′, respectively, and the length of PCR product is 538 bp. The PCR conditions were 35 cycles of denaturation at 94°C for 30 s, annealing at 68°C for 30 s, and elongation at 72°C for 30 s. iRFP transgenic mice will be available to the research community upon request.

Imaging of iRFP mice

The expression of iRFP was detected with an In Vivo Imaging System (IVIS Spectrum). iRFP expression was assessed in WT and iRFP mice at 8 weeks of age. All mice were anaesthetized with isoflurane or sacrificed before imaging. The hair on the backs of the mice was removed using a safety razor. The brain, heart, liver, kidney, spleen, lung, pancreas, teeth, bone, testis, thymus, and adipose tissue were harvested individually. These organs were imaged with IVIS.

Analysis of mouse body weight and blood indices

WT and iRFP male mice were used for these analysis. Body weight was measured at weeks 3 and 24 (Table1) after birth. Blood from 24-week-old (Table2) mice was collected in tubes containing EDTA then maintained on ice and immediately analyzed using a Celltac-α automatic hematology analyzer (NIHON KOHDEN). The serum concentrations of glucose, creatinine, GPT/ALT, cholesterol, and albumin were measured using an automatic blood analyzer (DRI-CHEM 7000, FUJIFILM Medical).

Reconstitution of iRFP hematopoietic cells

Recipient mice used for transplantation were generated in a BDF1 background. For hematopoietic cell reconstitution, 5×10^6 bone marrow cells were isolated from 8-week-old WT or iRFP mice, and these cells were injected into the tail vein of lethally irradiated (810 R) 6-week-old recipient mice. After 8 weeks, the chimerism of donor cells was examined by FACS analysis.

FACS analysis

The blood was collected in tubes containing EDTA and lysed with ACK buffer to destroy all red blood cells. Next, the cells were collected and washed with PBS. The cells were stained with several antibodies, such as Ter119 (eBioscience), B220 (eBioscience), CD3 (eBioscience), Gr1 (eBioscience), and Mac1 (eBioscience), for 1 h. Then, the cells were washed and suspended in PBS for analysis with a Gallios Flowcytometer (Beckman coulter).

Statistics

The data were calculated as the means ± SD. *t*-tests were used to compare the means, and analysis of variance was used to evaluate significant differences among the means. Significant differences were defined as $P<0.05$.

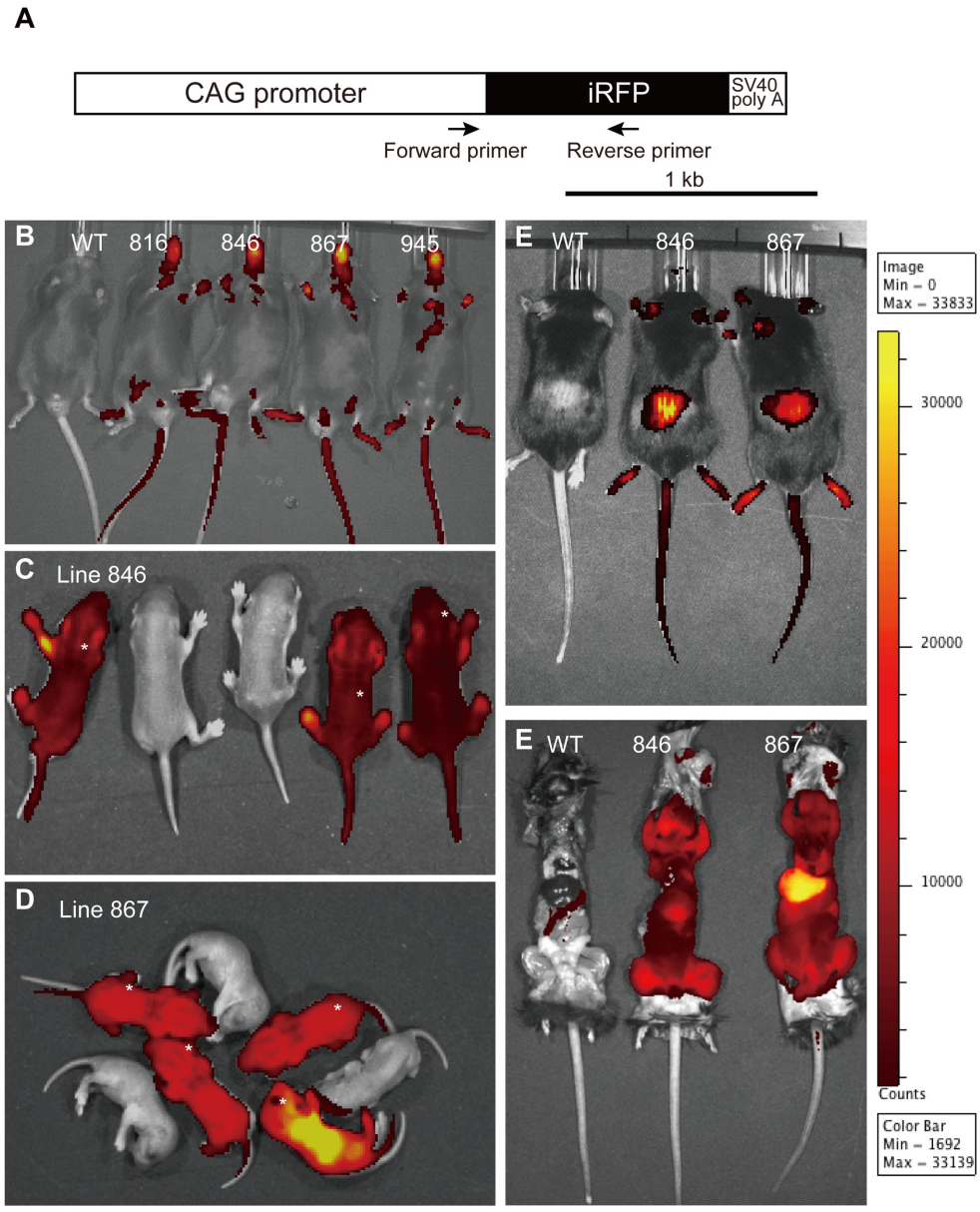

Fig. 1. Generation of transgenic iRFP mice. A: iRFP cDNA was fused to the CAG promoter. The arrows indicate the genotyping primers. B-F: iRFP mice were easily identified using an IVIS Spectrum system equipped with 710 nm excitation and 780 nm emission filters. B: Four lines of iRFP transgenic F0 mice and iRFP-negative WT. C: Newborn iRFP transgenic mice from line 846 (marked with an asterisk) and a WT littermate. D: Newborn iRFP transgenic mice from line 867 (marked with an asterisk) and a WT littermate. E: Whole-body imaging of WT and iRFP mice before autopsy. F: Imaging of whole organs from WT and iRFP mice.

Results and Discussion

Generation of iRFP expressing mice

We first inserted iRFP cDNA between a CAG promoter and SV40 polyA (Fig. 1A). This construct was injected into fertilized murine eggs. The iRFP mice expressed the infrared fluorescent protein, with an excitation peak at 690 nm and an emission peak at 713 nm. To develop iRFP transgenic mice, iRFP mice were crossed with wild-type (WT) mice. We obtained 4 lines of mice expressing iRFP: 816, 846, 867 and 915 (Fig. 1B). However, iRFP expression in line 816 was the weakest and

Table 1. Mean body weight of 3- and 24-week-old WT and iRFP transgenic mice

Mice	WT	Line 846	Line 867
Week 3	14.0 ± 0.7	14.4 ± 1.0	13.6 ± 0.8
Week 24	29.1 ± 1.0	28.5 ± 0.9	29.9 ± 2.5

Body weight of 3-week-old and 24-week-old WT and iRFP transgenic mice (n=8). The data indicate as the means ± SEM. There were no differences between WT and lines 846 or 867 (student's *t*-test).

Table 3. Serum indices of 24-week-old mice

Parameter	Mean ± SEM	
	WT	iRFP
Glucose (mg/dl)	244 ± 21.1	310 ± 30.3
Creatinine (mg/dl)	0.12 ± 0.0	0.1 ± 0.0
GPT/ALT (U/l)	24 ± 1.9	19 ± 1.8
Cholesterol (mg/dl)	68 ± 3.6	69 ± 11.3
Albumin (g/dl)	2.94 ± 0.1	3.02 ± 0.0

Mouse serum indices. The serum glucose, creatinine, alanine aminotransferase (GPT/ALT), cholesterol and albumin levels in transgenic fluorescent mice were not significantly different compared to WT mice (n=5). The data indicate the means ± SEM.

Table 2. Blood indices of 24-week-old mice

Parameter	Mean ± SEM			Range
	WT n = 5	Line 846 n = 6	Line 867 n = 4	
WBCs (× 10^2/μl)	87.0 ± 14.3	104.8 ± 5.3	88.3 ± 9.7	25–150
RBC (× 10^4/μl)	860.8 ± 20	902.7 ± 17	912.4 ± 27	650–1,250
HGB (g/dl)	13.3 ± 0.2	13.6 ± 0.3	13.85 ± 0.2	11.0–17.0
HCT (%)	44.9 ± 0.7	46.8 ± 0.9	46.7 ± 0.4	35–50
MCV (fl)	52.42 ± 0.3	51.8 ± 0.3	50.28 ± 1.0	45–60
MCH (pg)	15.6 ± 0.2	15.0 ± 0.1	14.9 ± 0.3	14–20
MCHC (g/dl)	29.7 ± 0.2	29.1 ± 0.1	29.7 ± 0.3	25–35.5
PLT (10^4/μl)	104.8 ± 8.2	100.7 ± 5.2	121.3 ± 6.7	60–150

Mouse blood indices. The blood indices of both transgenic mice and WT mice were within the normal ranges. The data indicate the means ± SEM.

line 915 did not transmit iRFP to offspring. Thus, we established 2 lines of mice that strongly expressed iRFP and transmitted the *iRFP* transgenic gene to their offspring: line 846 and line 867. WT mice were used as a control in this study.

Blood indices, body weight, and reproductive performance of iRFP transgenic mice

The health of mice needs to be considered for long-term applications of *in vivo* fluorescence imaging. In the present study, the mice were weighed at weeks 3 and 24 after birth, and the results indicated no differences between WT and iRFP mice (Table 1). The blood indices of iRFP mice were also within the normal range (Table 2). The serum levels of glucose, creatinine, GPT/ALT, cholesterol, and albumin were not different between WT and iRFP mice (Table 3). Moreover, difference were not observed between WT and iRFP mice in terms of organ morphology (Fig. 2 A'–L') or organ weight (Table 4). When mated the iRFP mice transmitted the transgenic genes to their offspring (Figs. 1C and D). In an analysis of the reproductive performance of iRFP mice, approximately 50% of the pups from the mating of WT female and iRFP male mice expressed iRFP. Taken together, these results suggest that iRFP expression does not affect body weight, organ weight, blood indices, or the reproductive performance of the transgenic mice (Table 5).

iRFP expression in the entire mouse body

First, the expression of iRFP was examined in the offspring. The entire bodies of the iRFP offspring exhibited fluorescence, whereas the control mice did not exhibited (Figs. 1C and D). The fluorescence intensity in line 867 offspring was higher than in the line 846 offspring.

Next, we detected fluorescence in adult mice. A small patch of hair was removed from the backs of the mice using a safety razor. Whole body imaging indicated that the shaved skin of iRFP mice displayed fluorescence, while unshaven skin did not. The tails, noses, forelimbs, and hindlimbs of these mice also expressed iRFP fluorescence (Fig. 1E). Then, the mice were sacrificed and

Table 4. Organ weight

Organ	Mean ± SEM	
	WT	iRFP
Brain (g)	0.52 ± 0.02	0.52 ± 0.02
Lung (g)	0.23 ± 0.01	0.22 ± 0.01
Liver (g)	1.26 ± 0.02	1.23 ± 0.03
Heart (g)	0.13 ± 0.01	0.13 ± 0.01
Spleen (g)	0.15 ± 0.01	0.14 ± 0.01
Kidney (g)	0.17 ± 0.03	0.14 ± 0.03

Weight of organs. Organs including the brain, lung, liver, heart, spleen and kidney of WT and iRFP mice were collected and weighted. The organ weights in iRFP transgenic mice were similar to those in WT mice (n=3). The data indicate the means ± SEM.

Table 5. Reproductive performance

	Pups			Mouse mother
	Total	WT	iRFP	
Line 867	26	13	13	3
Line 846	21	11	10	3

Reproductive performance. WT mice were mated with iRFP transgenic mice from line 867 and line 846. Approximately 50% of each group of pups expressed iRFP.

autopsied. All organs of the iRFP mice showed fluorescence by macro-scale observation (Fig. 1F).

iRFP expression in organs

Next, we harvested most organs for imaging, including the brain, heart, liver, kidney, spleen, lung, pancreas, teeth, bone, testis, thymus, and adipose tissue. In both mouse lines, the fluorescence intensity was similar among almost organs, but was higher in the lung, pancreas and especially liver. The fluorescence intensity in most organs from the 846 line was dimmer than 867 line (Figs. 2 A–L). These data suggest that the fluorescence intensity of line 867 is higher than line 846. Taken together, iRFP expression driven by the CAG promoter was observed in various organs.

Expression of iRFP in hematopoietic cells

Next, we examined the expression of iRFP in various blood cell types, including erythrocytes, granulocytes, monocytes, B cells and T cells. iRFP expression in the blood cells was evaluated after removing red blood cells, and the FACS data indicated higher iRFP expression levels in the blood cells of line 867 mice than line 846 mice (Fig. 3A). The fluorescence intensity ratios in the various types of blood cells were similar among WT, line 846 and line 867 mice, and the iRFP-positive cells expressed markers of erythrocytes, granulocytes, monocytes, B cells, and T cells (Figs. 3B and C). These results indicated that iRFP did not influence the population of hematopoietic cells.

To evaluate the reconstitution capacity of hematopoietic stem cells (HSCs) expressing iRFP, we generated mice expressing iRFP in the hematopoietic system by transplanting iRFP bone marrow (BM) cells into X-ray-irradiated mice. Two months after transplantation, we assessed the chimerism of the recipient mice. More than 70% of blood cells expressed iRFP in mice transplanted with iRFP HSCs (Fig. 4A). Moreover, the populations of erythrocytes, granulocytes, monocytes, B cells, and T cells were not different between WT control and iRFP-positive cells, as assessed by markers for different types of blood cells (Figs. 4B and C). These results indicate that the HSCs of the iRFP transgenic mice were able to reconstitute the hematopoietic systems of the irradiated mice. iRFP fluorescence was detected by the FL-7 (725/20) channel of a Gallios flow cytometer. Because this channel is infrequently used for FACS analysis, this channel is advantageous for multicolor flow cytometry analysis.

In light of the above findings, iRFP transgenic mice may represent a powerful tool for *in vivo* imaging after different types of transplantation experiments. For example, the iPS or STAP cells established from iRFP transgenic mice would exhibit NIR fluorescence after differentiation into various types of cells and tissues. Accordingly, this feature may enable researchers to investigate the involvement of iPS or STAP cells in regeneration processes in living mice in a non-invasive manner.

Acknowledgments

This work was supported by a Grant-in-Aid for Scientific Research on Innovative Areas “Fluorescence Live Imaging” from The Ministry of Education, Culture, Sports, Science, and Technology, Japan (23113502, 25113702), and by a Grant-in-Aid for Scientific Research on Priority Areas program. The work was also supported by grants from Scientific Research (S) (JSPS KAKENHI Grant Number, 21220009), and for JSPS Fellows (JSPS KAKENHI Grant Number, 24650228).

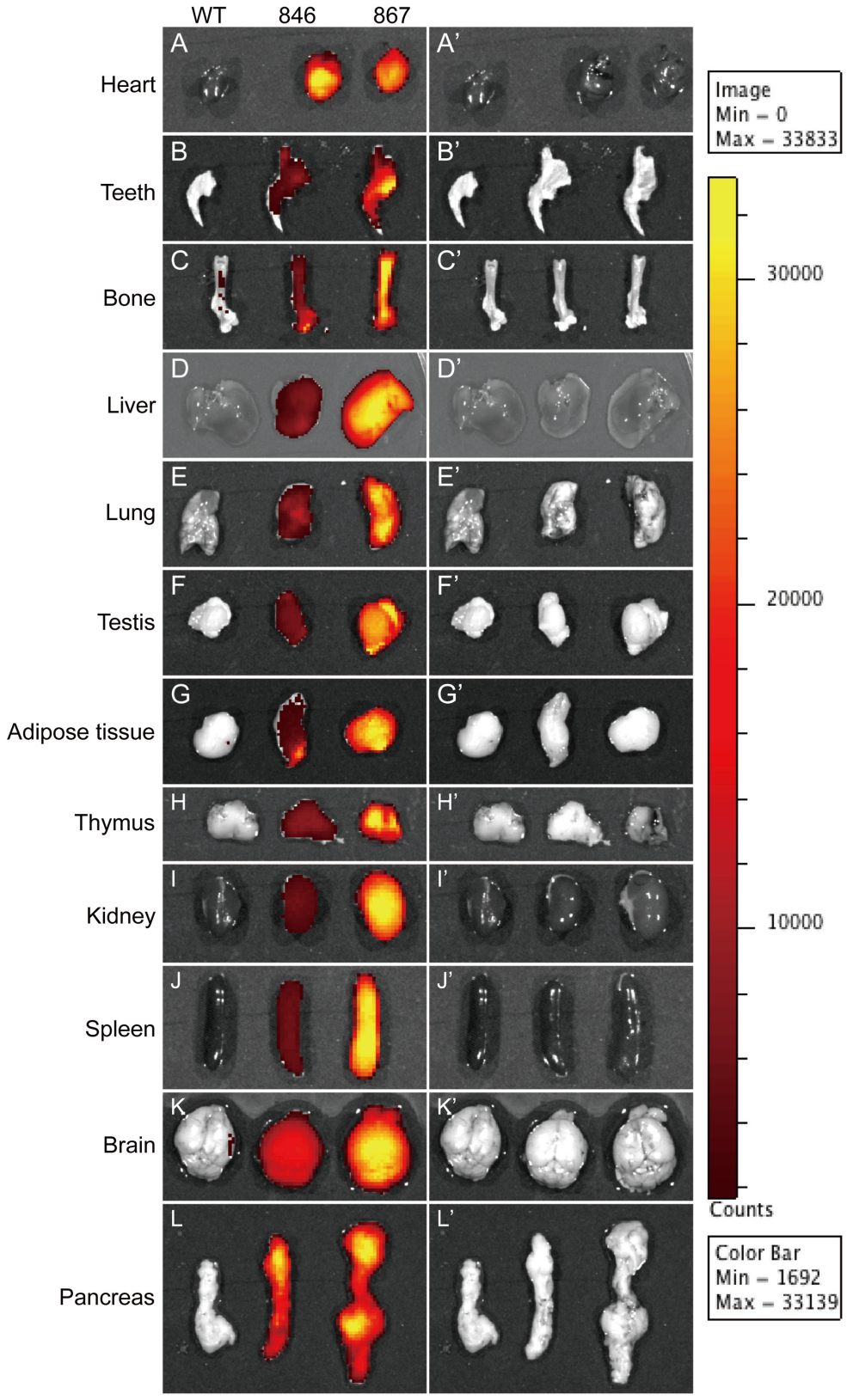

Fig. 2. iRFP is expressed in individual organs. A-L: Images under near-infrared light. A'-L': Images under visible light. Left, WT; middle, line 846; right, line 867.

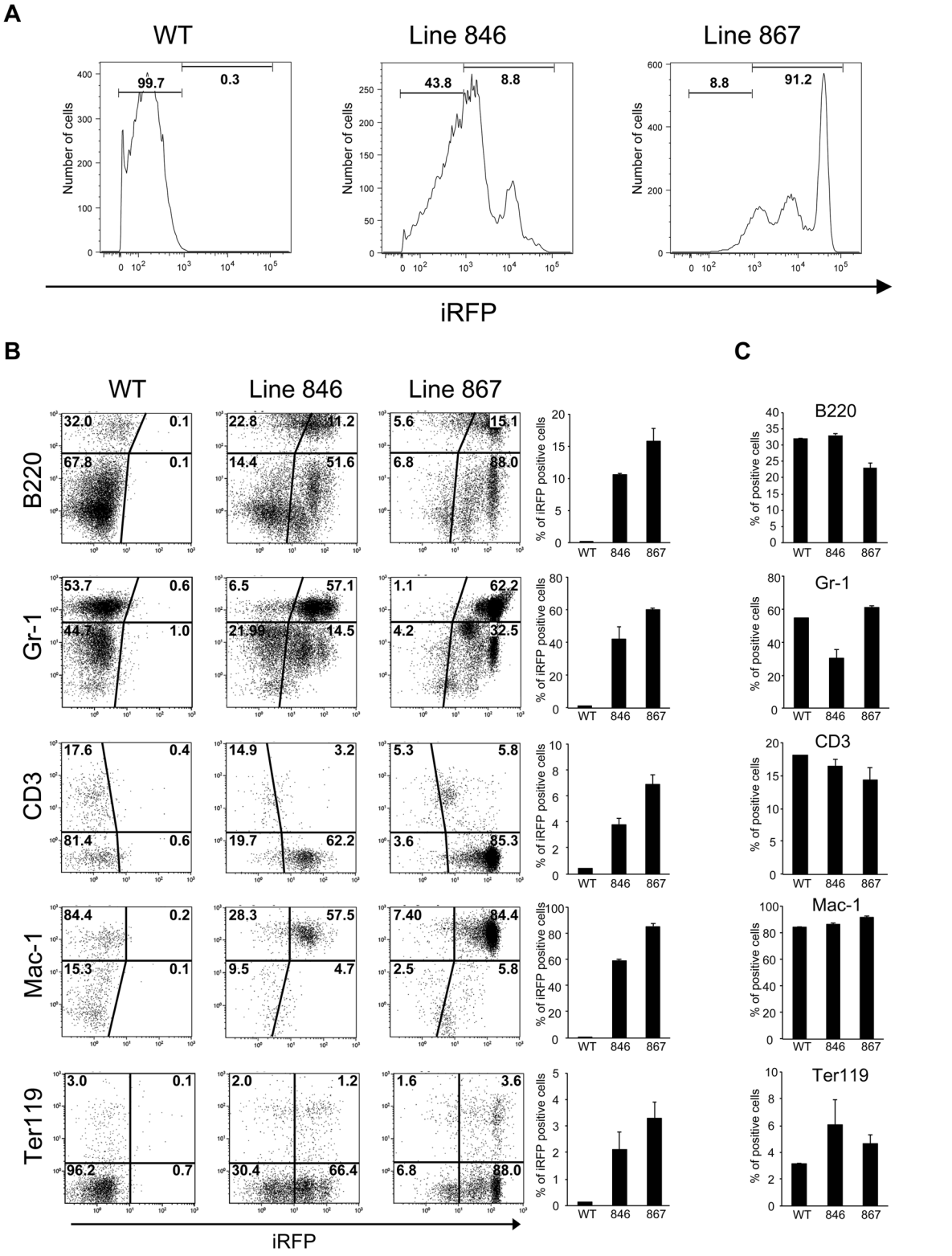

Fig. 3. Expression of iRFP in hematopoietic cells. A: Expression of iRFP in WT and iRFP hematopoietic cells after lysing red blood cells. B: FACS analysis of various blood cell markers (B220: B cell; Gr1: granulocyte; CD3: T cell; Mac1: monocyte; Ter119: erythrocyte). All blood cell types analyzed expressed iRFP. C: The expression of various blood cell markers in hematopoietic cells from WT and iRFP mice was similar. The data indicate as the means ± SEM. WT, n=4; lines 846 and 867, n=3.

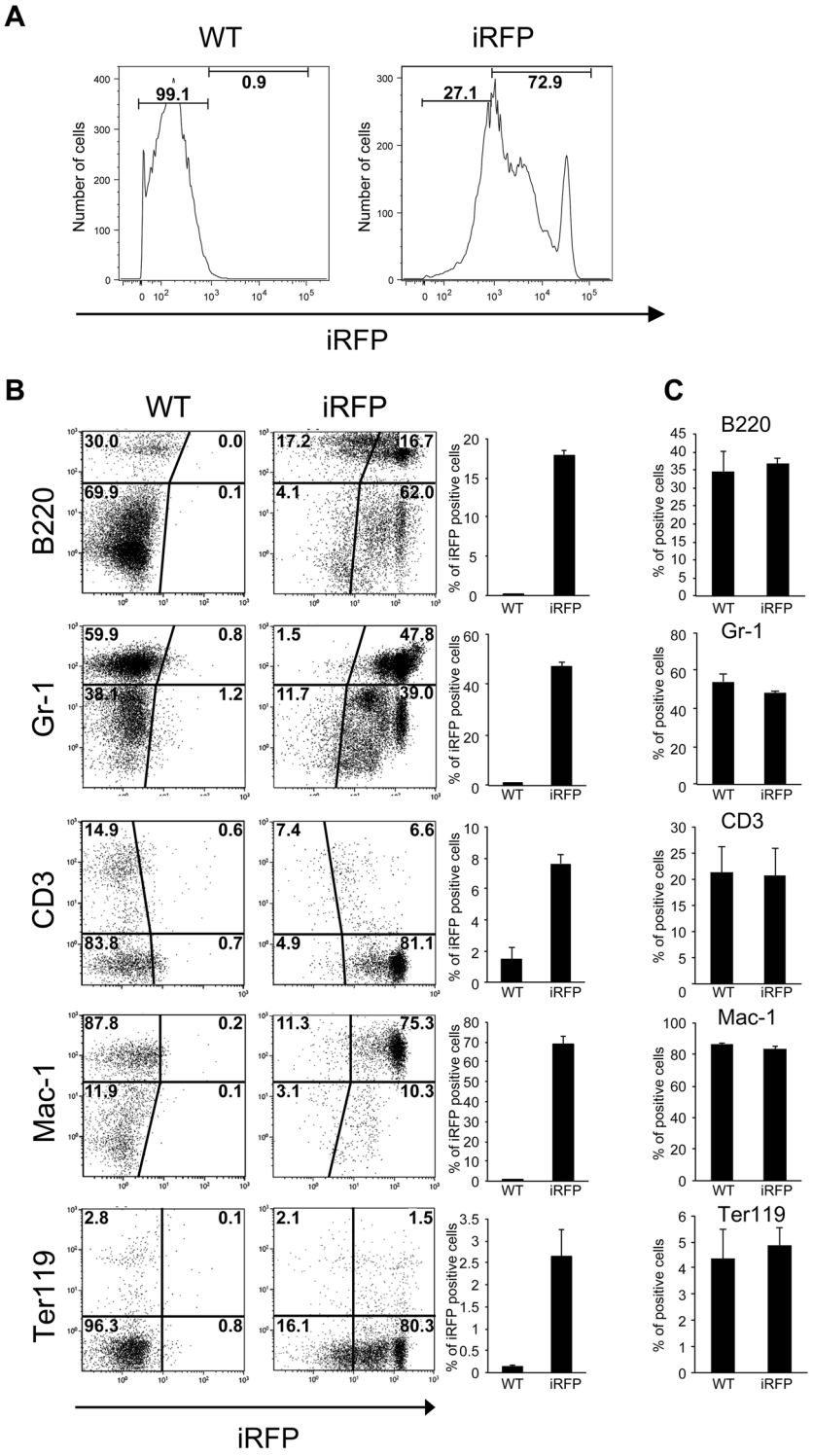

Fig. 4. Expression of iRFP in hematopoietic cells from BM cells-transplanted mice. A: Expression of iRFP in WT and iRFP hematopoietic cells after lysing red blood cells. B: FACS analysis of various blood cell markers (B220: B cell; Gr1: granulocyte; CD3: T cell; Mac1: monocyte; Ter119: erythrocyte). Most types of blood cells from mice transplanted with iRFP BM cells expressed iRFP. C: The expression of various blood cell markers in hematopoietic cells from WT and iRFP mice was similar. The data indicate as the means ± SEM. WT, n=3; iRFP mice, n=3.

References

1. Filonov, G.S., Piatkevich, K.D., Ting, L.M., Zhang, J., Kim, K., and Verkhusha, V.V. 2011. Bright and stable near-infrared fluorescent protein for in vivo imaging. *Nat. Biotechnol.* 29: 757–761. [Medline] [CrossRef]
2. Jöbsis, F.F. 1977. Noninvasive, infrared monitoring of cerebral and myocardial oxygen sufficiency and circulatory parameters. *Science* 198: 1264–1267. [Medline] [CrossRef]
3. Shimomura, O., Johnson, F.H., and Saiga, Y. 1962. Extraction, purification and properties of aequorin, a bioluminescent protein from the luminous hydromedusan, Aequorea. *J. Cell. Comp. Physiol.* 59: 223–239. [Medline] [CrossRef]
4. Shu, X., Royant, A., Lin, M.Z., Aguilera, T.A., Lev-Ram, V., Steinbach, P.A., and Tsien, R.Y. 2009. Mammalian Expression of Infrared Fluorescent Proteins Engineered from a Bacterial Phytochrome. *Science* 324: 804–807.
5. Tanaka, J., Miwa, Y., Miyoshi, K., Ueno, A., and Inoue, H. 1999. Construction of Epstein-Barr virus-based expression vector containing mini-oriP. *Biochem. Biophys. Res. Commun.* 264: 938–943. [Medline] [CrossRef]
6. Yamamoto, N., Tsuchiya, H., and Hoffman, R.M. 2011. Tumor imaging with multicolor fluorescent protein expression. *Int. J. Clin. Oncol.* 16: 84–91. [Medline] [CrossRef]